Multi-fidelity optimization strategy for the industrial aerodynamic design of helicopter rotor blades

Debbie Leusink[a,*], David Alfano[a], Paola Cinnella[b]

[a]*Airbus Helicopters, Aéroport Marseille Provence, 13725 Marignane Cedex, France*
[b]*Laboratoire DynFluid, Arts et Métiers ParisTech, 151 Boulevard de l'Hôpital, 75013 Paris, France*

Abstract

The industrial aerodynamic design of helicopter rotor blades needs to consider the two typical flight conditions of hover and forward flight simultaneously. Here, this multi-objective design problem is tackled by using a genetic algorithm, coupled to rotor performance simulation tools. The turn-around time of an optimization loop is acceptable in an industrial design loop when using low-cost, low-fidelity tools such as the comprehensive rotorcraft code HOST, but becomes excessively high when employing high-fidelity models like CFD methods. To incorporate high-fidelity models into the optimization loop while maintaining a moderate computational cost, a Multi-Fidelity Optimization (MFO) strategy is proposed: as a preliminary step, a HOST-based genetic algorithm optimization is used to reduce the parameter space and select a set of blade geometries used for initializing the high-fidelity stage. Secondly, the selected blades are re-evaluated by CFD and used to construct a high-fidelity surrogate model. Finally, a Surrogate Based Optimization (SBO) is carried out and the Pareto optimal individuals according to the SBO are recomputed by CFD for final performance evaluation. The proposed strategy is validated step by step. It is shown that an industrially acceptable number of CFD-simulations is sufficient to obtain blade designs with a significantly higher performance than the baseline and then SBO results issued from a standard Latin-Hypercube-Sampling initialization. The proposed MFO strategy represents an efficient method for the simultaneous optimization of rotor blade geometries in hover and forward flight.

Keywords: aerodynamics, optimisation, helicopter rotor blades

1. Introduction

The aerodynamic design of helicopter rotor blades has significantly evolved in the last fifteen years. Thanks to advances in simulation methods and increased computational capabilities, trial and error approaches (based on either simulation approaches of different degrees of complexity or on wind tunnel testing) [9], have been progressively replaced by automated design tools, which rely on the coupling of numerical models for rotor aerodynamics and automatic optimization algorithms.

Some of the early contributions to the automated design of helicopter blades were done at NASA Langley. Walsh et al. [31] automatically determined chord and twist distributions minimizing hover power consumption, with constraints on forward flight performance and stall conditions, by using the gradient-based optimizer CONMIN [1]. Rotor blade optimization was also carried out at ONERA [35], by coupling the CONMIN optimizer to the comprehensive rotor code R85 [6]. This optimization loop was used to maximize rotor performance in high-speed forward flight through the design of suitable airfoil shapes and of their spanwise distribution. This work was later extended by including CFD simulations in the optimization loop [8]: optimizations were aimed at maximizing rotor hover performance in terms of Figure of Merit (F.M.) by changing the twist distribution over the blade, as well as the chord, sweep and dihedral angle at the blade tip separately. Then, all geometrical parameters were combined into one optimization to optimize the ERATO blade for hover performance.

*Corresponding author. e-mail: debbie.leusink@airbus.com

The University of Bristol developed a similar optimization loop for rotor blades in hover, using an optimizer based on a nonlinear programming algorithm and CFD simulations for the flow analysis [3, 4]. Radial basis functions were used to manage mesh deformations induced by geometrical changes: this allowed ensuring high computational mesh quality; nevertheless, a large number of parameters was to be specified, even to perform a simple twist optimization [5]. A recent step forward in the automatic optimization of rotor blades in hover conditions using CFD was represented by the introduction of adjoint methods, which take into account gradients of the cost functions with respect to the design parameters [14]. This enables an efficient convergence of the optimization algorithm towards the nearest optimum, by using a small number of simulations.

Most of the above mentioned references focus on the optimization of rotor performance in hover flight only. However, for industrial applications, it is crucial to take into account in the design process forward flight conditions also. Optimization of a device for more than one operating condition is known as multi-point optimization (see e.g. [28]) and it naturally leads to the solution of a multi-objective problem. For gradient-based optimizers, a well-known approach for solving multi-objective problems is the weighted sum method, which combines (linearly or not) all of the objectives into a single cost function through the introduction of suitable weighting coefficients. An example of this kind of optimization strategy is represented by twist distribution optimizations of the 7A blade in hover flight carried out at ONERA using various optimization and simulation methods [20]. DLR also carried out gradient-based two-point blade optimizations using weighting coefficients for hover and forward flight conditions [17]: rotor performance predictions were obtained by means of CFD simulations weakly coupled to the comprehensive rotor simulation code HOST [10] to account for blade elasticity. An iterative procedure was required to couple the CFD and HOST codes, which increased computational cost significantly. The main shortcoming of these optimizations is the weighted-sum method, as this requires the selection of appropriate design points and their associated weights.

In parallel with the improvement of simulation tools for rotor performance evaluation, significant progress has been done on the optimization techniques themselves. These have evolved from optimizations using almost exclusively gradient-based algorithms, to more general multi-objective optimization algorithms. Specifically, considerable interest has been developed into genetic algorithms because of their capability to find global optima and to handle multiple objective functions. The increased cost associated with the loss of gradient-related information can be greatly alleviated by means of a straightforward parallel implementation.

For complex industrial applications, however, the number of cost-function evaluations required by genetic algorithms remains excessively high, especially when CFD simulation methods are used to compute the quantities of interest [24]. To circumvent this difficulty and drastically reduce the turn-around time of optimization cycles, advanced optimization techniques, such as optimization on a response surface and automatic updating of this surface in Surrogate Based Optimization (SBO) have recently been introduced in rotor optimization loops. For instance, Ref. [18] and [19] discuss a SBO based on the combination of a genetic algorithm with a Neural-Network reconstruction of the response surface from a limited number of CFD simulations for the optimization of dihedral and sweep distributions in forward flight.

Another strategy for reducing computational costs consists in generating a response surface based on both low- and high-fidelity simulation tools [12], as illustrated in Figure 1. Unfortunately, values of the objective function associated to a given blade geometry by low and high-fidelity simulation methods may differ significantly. Therefore, to integrate information from low- and high-fidelity simulations into a single surrogate model, the objectives are scaled by a factor that depends on the specific low- and high-fidelity models in use. The actual optimization is then performed on a metamodel which is built from low-fidelity simulations, combined with scaled high-fidelity simulations. Unfortunately, this technique only works when response surfaces associated to the low- and high-fidelity models only differ by a simple scaling, but their shapes are essentially the same. If this is not the case, the optimizer has trouble in identifying a suitable search direction toward the actual optimum.

An industrial application of two-point SBO at Agusta-Westland was discussed in [26]: a genetic algorithm was coupled with a panel method code to compute rotor performance in hover. The proposed methodology was demonstrated by simultaneously optimizing twist, chord and sweep laws for a rotor blade in two different forward flight conditions while constraining hover flight performance. In order to reduce the number of simulations required to evaluate rotor performance, a

surrogate model based on an Artificial Neural Network (ANN) was employed.

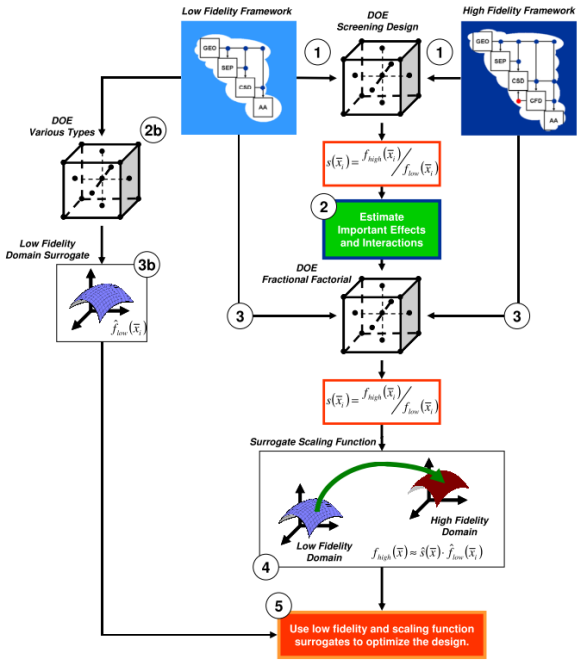

Figure 1: Combination of low- and high-fidelity simulation tools in Surrogate Based Optimization, from [12]

In the present work, we move a step forward in the two-point optimization of helicopter blades by incorporating cost-function evaluations based on a CFD model both for hover and forward flight conditions. To drastically reduce computational cost intrinsic to CFD simulations, we develop a two-step multi-fidelity optimization strategy, which blends together a multi-objective genetic algorithm, a surrogate model, and two different simulation tools for rotor performance evaluation, a low-fidelity, and a high-fidelity one. The former is the comprehensive rotor code HOST [10], which provides quick estimates of rotor performance based on a blade element method; the latter is the CFD code *elsA* [11]. The goal of the present work is to obtain a Pareto Optimal Front, from which one optimal blade geometry may be selected, taking into account for additional rotor blade design objectives, such as vibrations and acoustics.

The paper is organized as follows. Section 2 provides details of the low- and high-fidelity models. The design principles of the multi-fidelity optimization strategy are discussed in Section 3. Finally, the proposed methodology is applied to the optimization of the ONERA 7A blade, which was extensively investigated in wind tunnel tests [20].

2. Simulation tools for rotor performance prediction

2.1. Low-fidelity model: HOST code

The Helicopter Overall Simulation Tool (HOST) [10] is a comprehensive rotorcraft code developed at Airbus Helicopters. Aerodynamic forces are calculated by integrating the local lift as computed from 2D polars for small spanwise blade elements. The local velocity and angle-of-attack are obtained by adding the induced velocity to the local rotational and forward flight speed. Corrections for three-dimensional, transonic, Reynolds or sweep effects may be applied. Rotor equilibrium position is found by iteratively correcting blade positions in terms of pitch, flap and lead-lag angles according to the rotor loads. For the computations presented in the following, HOST simulations are performed using the Finite State Unsteady Wake (FiSUW) model [7] for modelling the induced velocity. This model was selected after a preliminary accuracy study described in [22].

HOST relies on a simplified physical representation of blade aerodynamics, but enables quick estimates of rotor performance. Specifically, the two-dimensional approach used in HOST simulations does not account for 3D effects, where the flow exhibits significant departures from an essentially (locally) two-dimensional flow. Moreover, in the aim of reducing computational costs, computations presented in the following do not take into account blade deformations (see [22] for a discussion).

2.2. High-fidelity model: elsA *CFD code*

The numerical flow solver *elsA* is developed at ONERA [11]. It solves the compressible Reynolds-Averaged Navier-Stokes (RANS) equations by means of a finite volume discretization on multi-block structured meshes. Given a mesh cell Ω, the RANS equations write:

$$\int_{\Omega} W_t d\Omega + \oint_{\partial\Omega} \bar{F} \cdot \bar{n} dS = \int_{\Omega} T d\Omega \qquad (1)$$

where W is the conservative variable vector, $\bar{F}$ is the flux density, including contributions from the inviscid

and viscous fluxes, and T is a source term including, e.g., the contribution of apparent forces. Several space and time discretization schemes are available, as well as a variety of eddy viscosity and Reynolds stress turbulence models. Here, we chose for the numerical approximation of convective fluxes an AUSM+ scheme with second order MUSCL extrapolation [25]. For turbulence modelling, the RANS equations are supplemented by Menter's SST $k-\omega$ turbulence model [27], which provides a reasonably good representation of turbulent shear stresses in boundary layers subject to an adverse pressure gradients. Both the turbulence model and discretization method were selected according to preliminary studies [22, 23].

Hover computations are carried out in the relative reference frame, and periodicity conditions are used to simulate only a single rotor blade. The numerical solution is driven to convergence towards the steady state by means of the Backward Euler implicit time integration scheme, combined with a deferred correction technique. The resulting system is solved by a LU-SSOR technique [32].

Forward flight computations require taking into account flow unsteadiness. To this aim, time accurate simulations are carried out by using a constant time step, corresponding to a change in azimuthal blade position by a quantity $\Delta\psi$. Time integration is done by means of the second-order backward difference scheme, given by:

$$\frac{1}{\Delta t}\left[\frac{3}{2}\mathbf{W}^{n+1} - 2\mathbf{W}^{n} + \frac{1}{2}\mathbf{W}^{n-1}\right] + \mathbf{R}_{\Omega}(\mathbf{W}^{(n+1)}) = 0 \quad (2)$$

where $\mathbf{R}_{\Omega}(\mathbf{W}^{(n+1)})$ is a numerical approximation of spatial terms in Eq. 1 and Δt is the integration time step. The nonlinear system of equations (2) is solved iteratively at each physical time step n by an approximated Newton method. For forward flight CFD computations, the rotor equilibrium of blade flapping, pitching and lead-lag motions are computed by HOST as a preprocessing step, and then imposed as an input for CFD calculations. In other terms, we do not use so-called weak coupling techniques, involving periodic updates of the rotor equilibrium conditions [8]. This would require several cycles of subsequent HOST and CFD simulations, increasing computational cost significantly.

2.3. Preliminary validations

To validate the simulation tools used in this study, various comparative studies are performed. At this stage, our objective is to assess the capability of HOST and *elsA* to discriminate between different blade geometries in terms of performance, both for hover and forward flight conditions, rather than providing accurate absolute performance predictions, since only trends of variation of the performance as a function of the design variables are required for optimization. To this aim, we consider three different blade geometries that were experimentally investigated at Airbus Helicopters [9]. Blade EC1 is a simple straight rectangular blade and represents the baseline geometry. Blade EC2 differs from EC1 by its twist distribution. Finally, EC3 differs from EC1 because of its chord law. Simulations are compared to performance measurements of these blades as gathered in the Modane wind tunnel for forward flight conditions. The blade performance is computed by HOST in terms of the lift-to-drag ratio L/D, whereas CFD simulations equivalently return the ratio of the rotor lift to the rotor torque coefficient, $\overline{Z}/\overline{C}$. Definitions of these performance measures are given in Section 3.1. In the following, we compare numerical and experimental results in terms of relative performance p with respect to the reference EC1 blade, i.e.:

$$p = \frac{p_{\mathrm{ECx}}}{p_{\mathrm{EC1}}} \quad (3)$$

A comparison of HOST computational results and wind tunnel measurements is given in Figure 2, while a comparison to CFD simulation results is given in Figure 3. These figures provide trends of the normalized difference in L/D and $\overline{Z}/\overline{C}$ as a function of the forward flight velocity Vh. Both simulation methods predict correctly that the modified twist law of EC2 has a negative influence on forward flight performance, when compared to EC1, in agreement with wind tunnel measurements. Concerning chord law modifications, both models predict a higher performance for the modified EC3 blade, similarly to wind tunnel results. More detailed validations of the low-fidelity and high-fidelity model are given in [22].

CFD computations in forward flight are based on a rotor equilibrium obtained from HOST. Yet, discrepancies between local flow fields obtained from both simulation methods increase with forward flight velocity due to differences in rotor equilibrium that are neglected in the present decoupled approach. For this reason, we chose to optimize the blades only at moderate forward flight velocities, where the effect of rotor equilibrium is negligible.

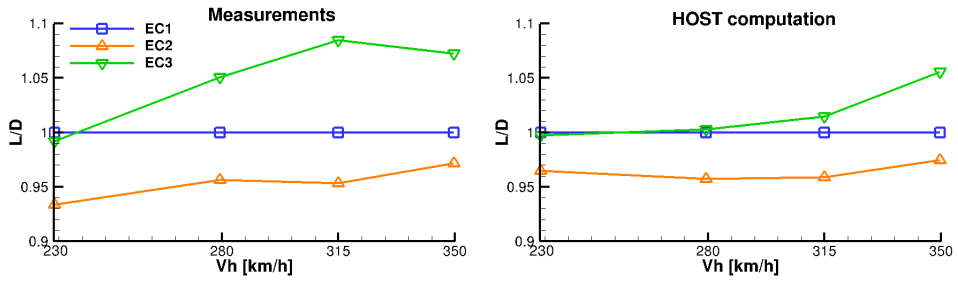

Figure 2: Forward flight performance for three blades, expressed in terms of the normalized aerodynamic efficiency L/D, versus the forward flight velocity. Left: wind tunnel measurements; right: HOST computations

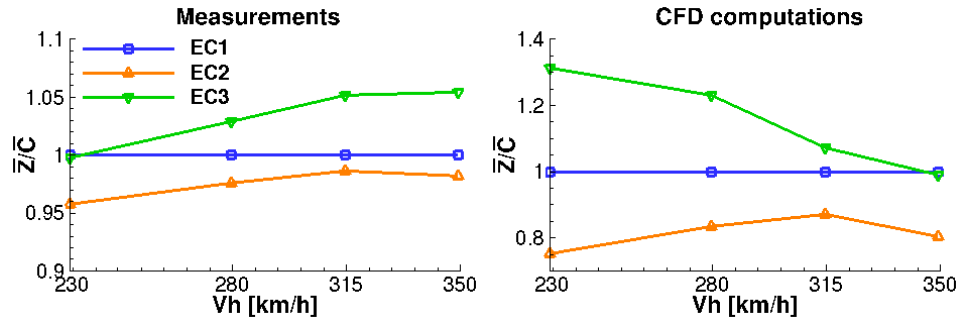

Figure 3: Forward flight performance for three blades, expressed in terms of the normalized $\bar{Z}/\bar{C}$ ratio, versus the forward flight velocity. Left: wind tunnel measurements; right: CFD computations

3. Optimization strategy

3.1. Problem definition

Our goal is to find rotor blade geometries that simultaneously optimize hover and forward-flight performance. To this aim, a pair of relevant hover/forward flight operating conditions is selected. Rotor performance in hover is quantified by means of the Figure of Merit (F.M.). This is defined as the ratio of ideal rotor power P_{ideal} as calculated by Froude [16, 21] to the actual rotor power P:

$$F.M. = \frac{P_{\text{ideal}}}{P} = \frac{C_T^{3/2}}{\sqrt{2}C_P} \tag{4}$$

where the rotor thrust coefficient C_T is defined as:

$$C_T = \frac{T}{\rho A V_{\text{tip}}^2} = \frac{T}{\rho A \Omega^2 R^2} \tag{5}$$

and rotor power coefficient C_P, based on the induced and profile power, is expressed as:

$$C_P = \frac{P}{\rho A V_{\text{tip}}^3} = \frac{P}{\rho A \Omega^3 R^3} \tag{6}$$

In Equations (5) and (6), T is the rotor thrust, ρ the free-stream density, A the rotor disk surface, V_{tip} the blade tip speed and R the rotor radius. The F.M. indicates how efficiently the rotor generates the power necessary to hover, i.e. takes into account the impact of aerodynamic losses on rotor power generation. Our objective is then to find rotor blade geometries that provide the highest possible F.M. for a given rotor loading in hover, defined as:

$$\bar{Z} = \frac{F_z}{\frac{1}{2}\rho b \bar{c} R V_{\text{tip}}^2} \tag{7}$$

where F_z is the rotor lift, b the number of blades and $\bar{c}$ the mean aerodynamic chord of a blade.

Rotor performance in forward flight is quantified

through the aerodynamic efficiency L/D of the rotor:

$$\frac{L}{D} = \frac{T\cos\alpha}{P/V_\infty} \approx \frac{WV_\infty}{P} \tag{8}$$

where α is the inclination angle of the tip path plane, i.e. the plane formed by the blade tips, with respect to the axis perpendicular to the rotor hub. As α is small in stabilized forward flight, then $\cos\alpha \simeq 1$ and $T\cos\alpha$ may be approximated as the helicopter weight W.

Alternatively, forward flight performance can also be measured in terms of the ratio of rotor lift to rotor torque coefficients: $\bar{Z}/\bar{C}$, since the rotor power consumption is directly proportional to rotor torque Q for a specific flight condition with rotor loading $\bar{Z}$. Precisely, the rotor torque coefficient is defined as:

$$\bar{C} = \frac{Q}{\frac{1}{2}\rho b\bar{c}RV_{\text{tip}}^2} \tag{9}$$

Rotor torque is also considered as forward flight performance measure in [17]. For either of the two forward flight performance measures, the objective is to identify a rotor geometry with the highest aerodynamic efficiency for a given forward flight velocity.

In practice, hover and forward-flight performance often lead to conflicting requirements on blade geometry. As a consequence, the final design will generally represent a trade-off between both conditions.

To achieve this, we formulate a multi-objective optimization problem of the form:

Find the set of $\mathbf{s}$ *such that hover and forward flight performance are simultaneously maximized* (10)

to find a Pareto Optimal Front where $\mathbf{s} \in S$ is the vector of design parameters describing the blade geometry, S being the set of admissible geometries.

3.2. Parameterization of the blade geometry

A family of blade geometries is generated by defining analytical expressions for the twist and chord laws. The airfoil section is supposed to be the same all along the blade span. No attempt is made to optimize the sweep law, since this would require taking into account complex multi-disciplinary constraints. Similarly, we deliberately exclude from the automatic optimization procedure the blade root and tip regions, for which the simulation tools in use are still not predictive enough.

Twist and chord laws are parameterized by Bézier curves with 6 control points at fixed radial positions along the blade span. Ranges of variation of control points are depicted on the y-axis of Figure 4 both for twist and chord laws. These parameter ranges are selected to include ONERA's 7A blade, used in the following application. A geometrical constraint is imposed on the mean aerodynamic chord, required to be within 0.13 and 0.15m. As a result of the parameterization, the solution of the optimization problem requires the definition of 12 design parameters, represented by the y-axis values of Bézier control points for twist and chord laws.

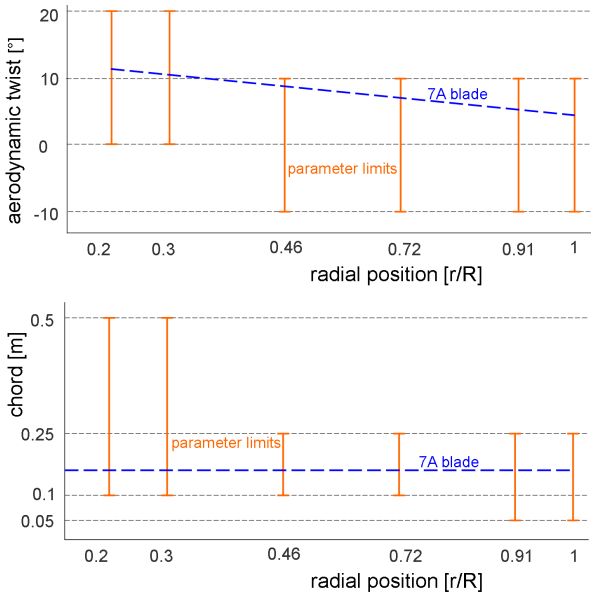

Figure 4: Parameter ranges for twist (top) and chord (bottom) laws

3.3. Optimizer and response surface modeller

In this work we adopt a genetic algorithm (GA) as the optimizer. This choice is motivated by its capability of locating globally optimal solutions for multi-modal problems, of finding the Pareto Optimal Front for multi-objective problems, and by its non-intrusiveness, which opens the way to coupling with a variety of simulation tools. All of these properties make GAs well suited for the industrial optimization of rotor blades, which naturally leads to the solution of multi-objective, multi-modal problems. Precisely, the optimizer used for the present computations is the Multi-Objective Genetic Algorithm (MOGA) available in the open source

Dakota optimization library [1]. It can be coupled in a straightforward way with both the low- and high-fidelity model. In the following, the GA is run with an initial population of 80 individuals, which is let to evolve over approximately 20 generations. The population can be initialized randomly (initialization from scratch) or from a pre-defined set of geometries, for instance based on a preliminary design of experiments. The MOGA available in DAKOTA uses a variable number of individuals in each generation. With the setup described above, the order of magnitude of cost-function evaluations required by an optimization run is of the order of 1000.

For a low-fidelity model, this number is considered to be acceptable because a complete optimization run can be executed overnight. On the contrary, when computationally intensive models are used to evaluate the cost functions, the turn-around time of the whole optimization process may become unacceptably high, especially in an industrial context. For instance, a complete CFD-based GA-optimization would have to a turn-around time of several months.

To circumvent this difficulty, Surrogate-Based Optimization is adopted to reduce computational costs. SBO requires the construction of an analytical model relating design variables and cost functions, called a *surrogate model*, or *response surface*, based on a preliminary sampling of the design space. Model construction is done according to a predefined criterion. This is called a Design of Experiment (DoE). An efficient surrogate model should be able to provide an accurate representation of the design space by using a minimal number of samples.

In this work, the DoE is carried out using Latin Hypercube Sampling (LHS): the parameter space is discretized by a uniform grid of points, then a subset of points is selected for cost-function evaluation [13]. Precisely, we randomly extract a subset of 80 points, from a grid of the same number of points in each direction. Then, a surrogate model is constructed from the sample through a Gaussian Process (GP) modelling technique [1, 30]: data from the initial sample are interpolated through a multivariate normal distribution. Precisely, the GP is built as a linear combination of shape functions $\mathbf{B}_j$ plus a local correction term given by the error function $z(\mathbf{x})$ [1, 15, 34]:

$$\hat{f}(\mathbf{x}) \approx \sum_{j=0}^{L} \beta_j \mathbf{B}_j + z(\mathbf{x}) \tag{11}$$

In Eq. 11, the $\mathbf{B}_j$ are polynomial functions of order L and the β_j are linear combination coefficients. The first term in the right-hand side of Eq. 11 is meant to capture large scale variations of the response surface; error function $z(\mathbf{x})$ is a stochastic process with zero mean, variance σ^2 and covariance described by a Gaussian correlation function, and it accounts for local fluctuations with respect to the shape functions. The order of the polynomials functions L Details of the formulation for $z(\mathbf{x})$ are given in [1, 29, 34]. These models are expected to predict accurately highly nonlinear and irregular function behaviours [33].

The surrogate model is finally coupled with the optimizer. Periodic updates of the surrogate during the optimization process may be carried out to improve its accuracy as the optimization converges toward the optimum.

3.4. Setup of the Multi-Fidelity Optimization strategy

In this Section, we propose a Multi-Fidelity Optimization (MFO) strategy, which aims at combining the quick and wide exploration capabilities of the design space of the low-fidelity model combined to a GA, with the greater accuracy of the high fidelity tool.

The MFO is made up of four subsequent steps.

Step 1. A preliminary exploration of the design space is carried out by using the low-fidelity model coupled to the GA. The non-dominated geometries resulting from this initial step are, in general, not optimal for the high-fidelity model. Nevertheless, the low-fidelity model is considered as reliable enough to exclude regions of the parameter space leading to too low fitness values.

Step 2. Based on the results of Step 1, the variation ranges of design parameters are reduced in order to exclude low-fitness regions. The advantage of working on a reduced design space is the possibility of achieving a more accurate construction of the response surface for a given population size.

Step 3. Compute rotor performance of a subset of geometries extracted from the low-fidelity step with the high-fidelity tool. Precisely, the sample of designs used to construct the surrogate model is composed by the blades having improved performance with respect to the baseline design, but are not necessarily Pareto optimal, in order to ensure a good diversity of the sample.

Step 4. A high-fidelity surrogate model is constructed on the reduced parameter space using the results of Step 4.

Step 5. Finally, a SBO is run on the high-fidelity-based surrogate model. The initial population is composed by the blade geometries selected in Step 3, from the low-fidelity optimization. To reduce computational cost, the surrogate model is not updated during the optimization.

The MFO strategy is schematized in Figure 5.

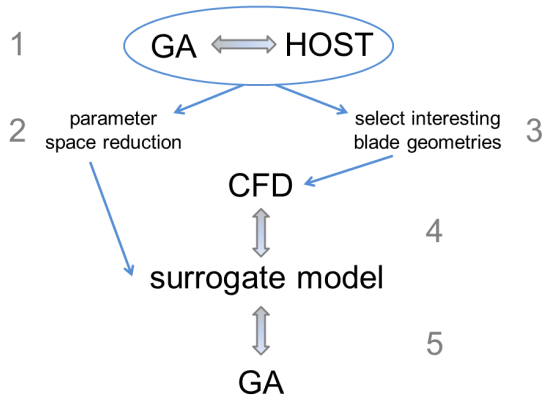

Figure 5: Multi-Fidelity Optimization strategy for rotor blade optimization using HOST and *elsA*

4. Application to the optimization of the 7A blade

In this Section we apply the proposed optimization strategy to improve the performance of the 7A blade. This blade, designed by ONERA, has a radius of 2.1m and uses OA2XX airfoil sections of 13 and 9% relative thickness. The rectangular blade has a chord of 0.14m and a linear aerodynamic twist variation. The blade has been extensively investigated and is often used for optimization studies, for instance in [2, 17, 20].

We select the following hover and forward-flight conditions as the optimization points:

- in hover, the rotation speed equals 1014 rot/min and all computations use a collective pitch angle that corresponds to maximum F.M. of the 7A reference blade;
- in forward flight, the design point is fixed at moderate forward flight speed μ=0.3 (where μ is the advance parameter defined as the ratio of the forward flight speed with respect to the rotational speed at the blade tip $\mu = V_H/\Omega R$); and moderate blade loading ($\overline{Z} = 15$).

Several optimizations are performed to validate the optimization loop.

4.1. GA and SBO optimizations with HOST

First of all, we validate the SBO methodology against a full GA optimization, taken as a reference. In both cases, cost-function evaluations are based on the low-fidelity model only.

The reference is obtained by running the MOGA over 20 generations, with a population composed of 80 individuals. We assume that convergence is achieved when performance improvement for both objectives is less than 0.5% over the last 5 generations. Figure 6 shows the resulting Pareto optimal front (POF).

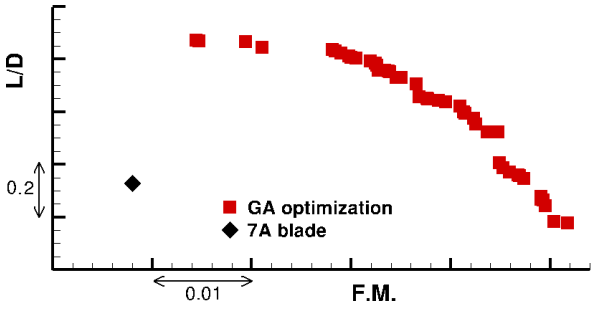

Figure 6: Pareto Optimal Front of the full GA, HOST-based optimization

Twist and chord laws associated to Pareto-optimal individuals from the full GA optimization are illustrated in Figure 7. The curves are coloured by the corresponding F.M. value. Blades with high twist gradients and hyperbolic laws exhibit better hover flight performance, as predicted by blade element theory [21]. On the contrary, nearly linear, low-gradient twist laws lead to better forward flight performance. Concerning chord distributions, the best forward flight performance is provided by blades with a low chord section near the blade tip and, more in general, a globally lower mean chord. Conversely, blades with high hover flight performances exhibit an increased chord throughout the span and more particularly at the blade tip.

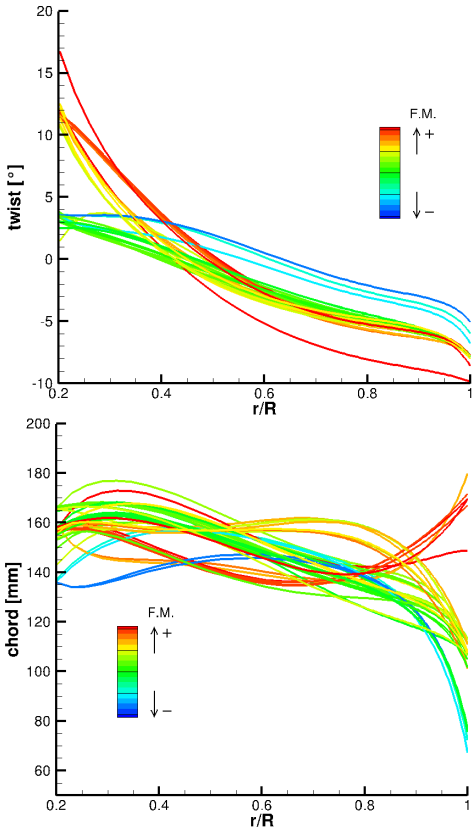

Figure 7: Blade geometry laws of GA-optimized blades, coloured by HOST-computed F.M. values

Then, a SBO optimization is performed using 80 blade geometries for initial response surface generation and 5 subsequent metamodel update steps consisting of 20 added blade geometries. In total, 180 blade geometries are simulated within the SBO, compared to 1600 for the full GA. Fig. 8 compares the Pareto-optimal front for the full GA optimization and the approximated Pareto-front provided by the SBO with the above mentioned parameter setting. Cost function values associated to optimal designs for the SBO have been recalculated with HOST. A reasonable agreement is observed, even if the SBO does not capture the whole extent of the POF (some favourable configurations for hover flight are missing in the SBO optimization). All of the SBO non dominated individuals represent a significant improvement over the baseline configuration.

Solutions obtained with the SBO algorithm display similar geometrical features: namely, the mean aerodynamic chord is reduced for high forward flight performance individuals. Unfortunately, the algorithm misses part of the blades with high hover performance (characterized by a high mean chord value). Nevertheless, since the optimal design is in general chosen in order to get a good trade-off between the two objectives, we consider that missing part of the high F.M. portion of the POF is an acceptable price to pay to achieve a reduction in computational cost.

Significant reductions in the number of cost-function evaluations do not completely justify the use of the SBO for HOST-based optimizations, but do represent a good trade-off between cost and accuracy for high-fidelity optimizations, as shown in the following.

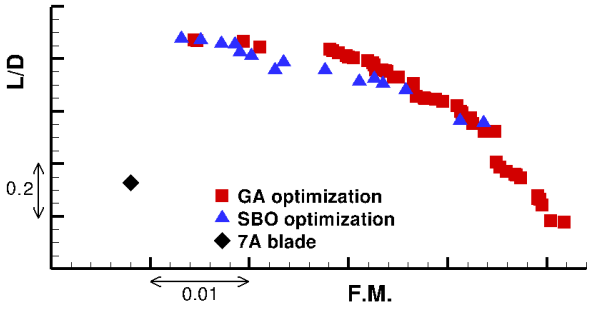

Figure 8: Pareto Optimal Fronts of GA and SBO optimizations, compared to 7A blade performance. Cost function evaluations are based on the HOST code

4.2. Multi-Fidelity Optimization

The low-fidelity GA-HOST optimization discussed in the preceding Section is used in the MFO strategy for a preliminary exploration of the design space. This serves two purposes: first, it is used to reduce the parameter space by excluding low-performance regions; on the other hand, values of design variables corresponding to "interesting" blade geometries are used in the high-fidelity stage for surrogate model construction and SBO initialization.

To reduce the parameter space, the evolution of rotor performance during the optimization is studied as a function of the design variables. For instance, Figures 9 and 10 show variations the F.M. in hover and of L/D in forward flight as functions of twist angle at blade tip and of the blade chord at a radial position corresponding to 0.46 R. Optimal twist at the blade tip tends clearly to be clustered in the range $[-10, -5]$ as the algorithm converges, so that the parameter space can be greatly restricted around these optimal values. Conversely, no

clear trend is observed when looking at performance parameter as functions of the chord at 0.46R: in this case, best fit results are clustered around two different chord values, corresponding approximately to 0.12 and 0.17m. The parameter range is in this case reduced to [0.12,0.20], corresponding to a diminution of only 20% with respect to the initial choice, to include both types of blade geometries. In a similar way, the parameter range of all other design variables is reduced. Precisely, the modified parameter intervals contain 90% of the blades of the last 5 generations. This method leads to an overall parameter space reduction of about 40%.

The subsequent step of the MFO strategy consists in using selected designs from those generated during the low-fidelity step to construct the CFD-based response surface. This set is chosen in such a way as to represent a large diversity of blade geometries and to lead to a good quality surrogate model within this region of interest.

Optimization evolution in the objective space is shown in Figure 11. The first 4 generations are composed by widely spread individuals and correspond to the initial exploration of the design space. From the 6^{th} generation on, the algorithm detects the correct direction for maximizing both objectives simultaneously. From this generation on, the Pareto Front is approached and solutions are refined. To initialize the CFD-based response surface on a large set of interesting designs, generations 6 and 10 are selected. Their twist and chord laws are compared to HOST-based POF blades in Figure 12. Both for chord and twist laws, generations 6 and 10 contain a large variety of geometries, encompassing the HOST-based optimal blades.

The performance of the selected low-fidelity blades (106 geometries in total) is then evaluated by CFD. Hover and forward flight performance efficiencies are expressed, as anticipated, in terms of F.M. and $\overline{Z}/\overline{C}$, respectively. Figure 13 shows that a significant number of the selected blades exhibits better rotor performance at both flight conditions with respect to the reference blade.

The selected sub-set of geometries is used to construct a CFD-based surrogate model for the subsequent optimization step. Figure 14 shows optimal blade geometries resulting from SBO. For both twist and chord laws, design parameters associated to the optimized blades are well within the set of geometries used for metamodel construction, so that errors introduced by the surrogate model can be assumed to be small.

Figure 15 presents CFD results for the Pareto-optimal

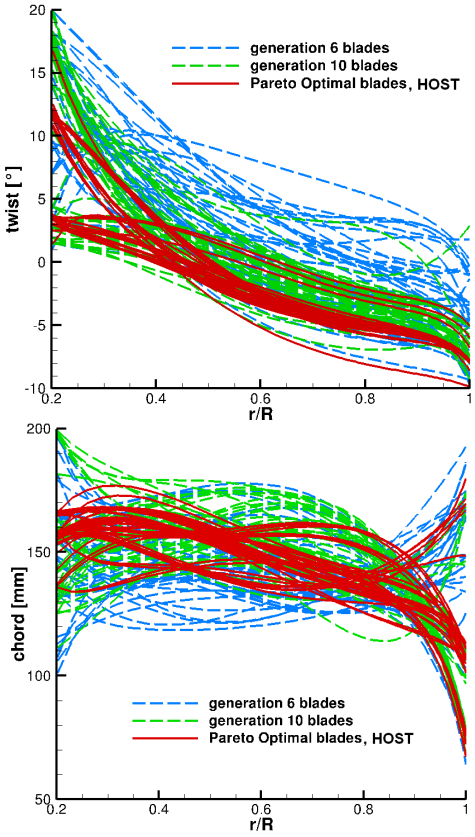

Figure 12: Blade geometry laws of low-fidelity selected blades, compared to Pareto Optimal blades issued from the low-fidelity step using HOST

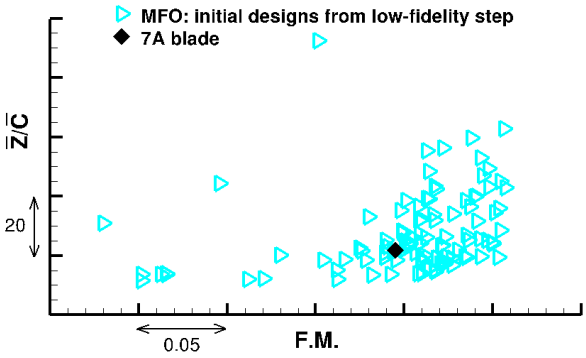

Figure 13: CFD computation results of surrogate construction for high-fidelity phase

blades issued from the SBO. CFD results for the initial design of the SBO and for designs belonging to the

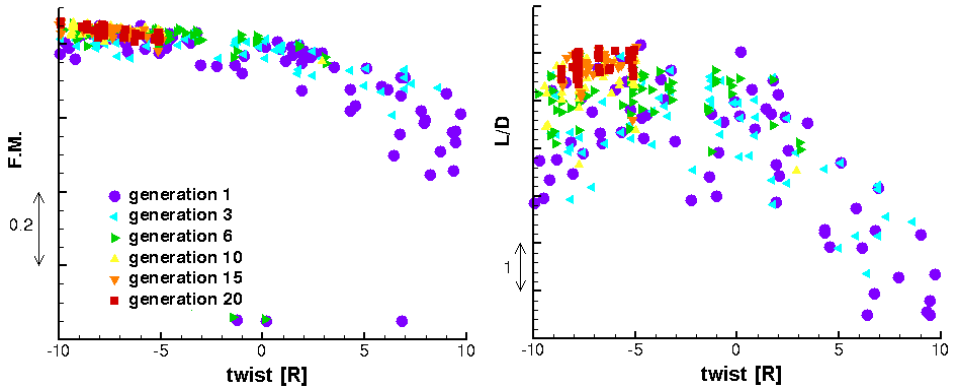

Figure 9: Plot of the hover performance in terms of F.M. (left) and forward flight performance in terms of L/D (right) as functions of the twist angle at the blade tip, GA optimization with HOST

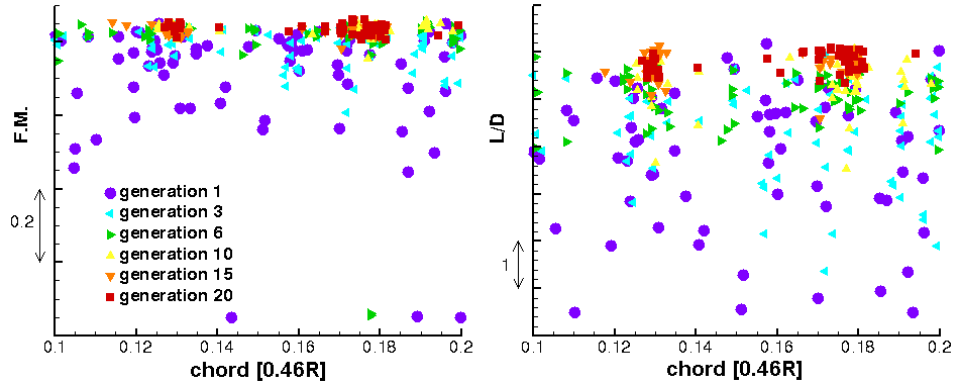

Figure 10: Plot of the hover performance in terms of F.M. (left) and forward flight performance in terms of L/D (right) as functions of the blade chord at radial position 0.46R, GA optimization with HOST

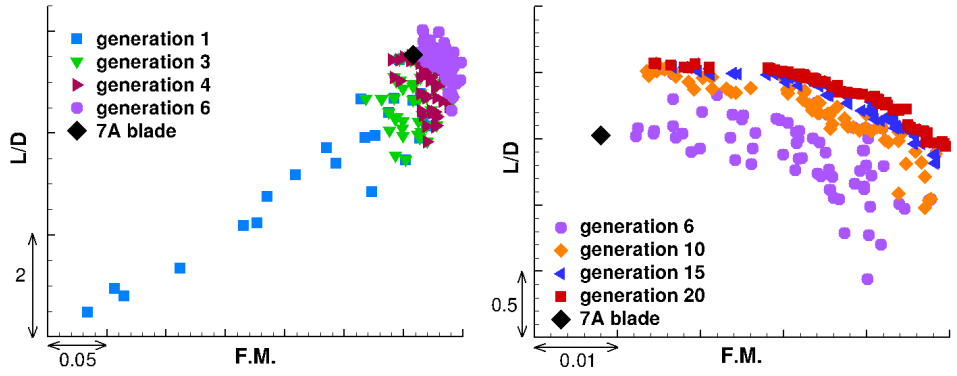

Figure 11: Evolution of the HOST-based genetic algorithm optimization at successive generations

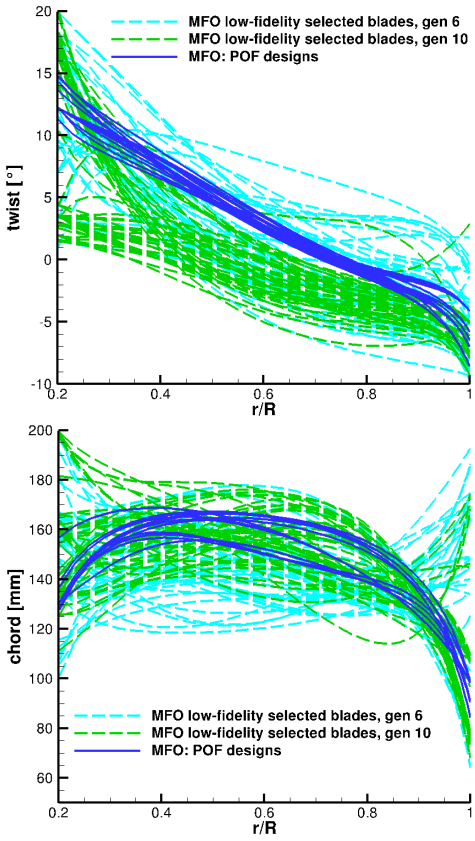

Figure 14: Blade geometry laws of high fidelity SBO optimized blades

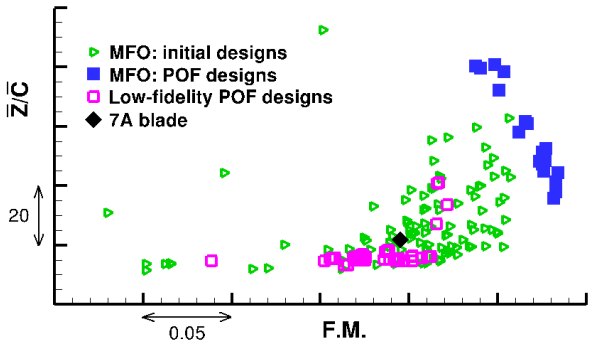

Figure 15: Comparison in the objective space of POF designs obtained after SBO against POF designs obtained after the low-fidelity step. Designs used to initialize the SBO are also represented for reference. CFD computations

low-fidelity POF are also represented for comparison. It is observed that, according to the high-fidelity CFD model, blades issued from the SBO stage have a much better overall performance than blades generated by the low-fidelity model.

To demonstrate the advantages of the proposed MFO strategy, the preceding results are compared to those of a standard CFD-based SBO using a random initialization of the full parameter space. As in the previous case, 106 blade geometries are generated, this time by means of LHS, and evaluated by CFD. The initial values of the cost functions for both high-fidelity initialization methods are compared in Figure 16: a larger number of initial designs obtained via the MFO strategy demonstrate a fitness improvement with respect to the reference geometry, compared to the initial designs generated by the LHS strategy. Note however that the LHS initialization includes a higher number of designs with high forward flight performance in terms of $\bar{Z}/\bar{C}$, corresponding to geometries that were apparently considered non-optimal in the low-fidelity phase.

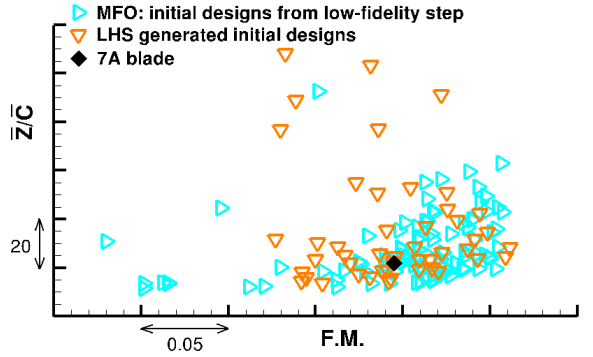

Figure 16: CFD computation results of initialization based on MFO and LHS strategy

Figure 17 compares POF designs issued from both SBO strategies. Twist distributions are found to be very similar for the two strategies, except in the outer part of the blade. Chord laws, however, are significantly different. Blades optimized by the MFO strategy show concave double taper laws, whereas LHS strategy optimized blades exhibit convex taper and thus increased chord sections near the blade tip. This is due to the fact that different choices of the initial set of geometries lead to different response surfaces and, consequently, to different designs.

Figure 18 compares the Pareto Optimal Fronts obtained by both optimization strategies. Clearly, designs obtained by applying the MFO strategy dominate POF

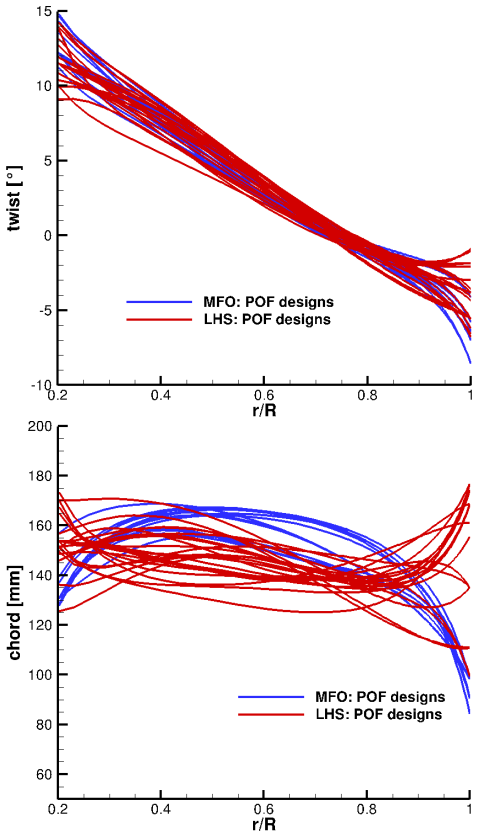

Figure 17: Blade geometry laws of MFO and LHS strategy SBO optimized blades

designs provided by the LHS SBO. The reason is that designs used to construct the surrogate model in MFO are closer to the region of interest, and the resulting approximation of the response surface is more accurate. On the other hand, the LHS strategy finds blade geometries with very good forward flight performance but provides designs with lower hover performance than MFO. Now, for industrial applications, the central zone of the Pareto Optimal Front is the most important one from a practical viewpoint, because it represents trade-off solutions between the different objectives. Therefore, even if MFO strategy misses the high forward flight performance part of the POF, this is not critical: on the contrary, thanks to the preliminary design selection in the low-fidelity phase, the MFO strategy converges efficiently toward the best trade-off solutions. The forward shift of the POF obtained with the MFO strategy with respect to that issued from a standard LHS initialization illustrates the effectiveness of the proposed method in finding a better approximation of the actual CFD POF for a given computational cost.

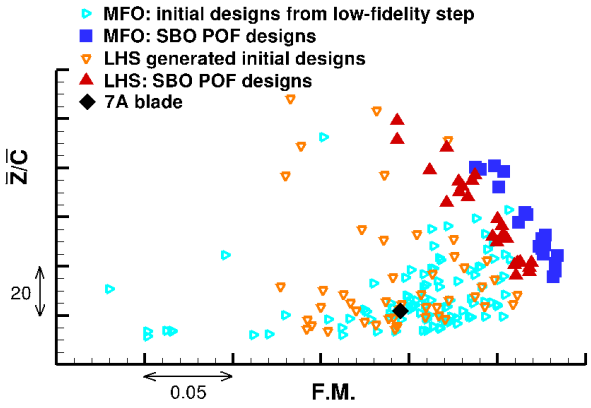

Figure 18: Comparison of SBO results obtained by using the MFO strategy and a LHS initialization. CFD computations

5. Conclusions

The aerodynamic optimization of helicopter rotor blades is a particularly difficult design problem due to the radically different features encountered in the two typical flight conditions of hover and forward flight. In this work, a genetic algorithm (GA) was chosen as the optimizer, because of its ability to handle intrinsically multi-objective design problems. The drawback of a GA is that it requires a high number of objective function evaluations. This is acceptable for industrial application when using a low-cost simulation tool, such as the comprehensive rotorcraft code HOST, but it leads to unacceptably high computational costs when coupled to high-fidelity CFD tools. A strategy for incorporating high-fidelity CFD information in the optimization loop, while conserving a moderate computational cost is proposed and analyzed. Results are used to reduce the design space to a region of high performance designs according to this model, but still large enough to allow for an effective search during the subsequent high-fidelity step. A set of “interesting” blade geometries is selected among the designs explored in the low-fidelity step, and is used to initialize the high-fidelity phase. In the second stage, rotor performance of these selected blades is computed by CFD to generate a surrogate model on which the actual optimization is performed.

The proposed multi-fidelity optimization approach is applied to the optimization of the 7A blade for hover

and forward flight conditions simultaneously. The MFO strategy is shown to generate designs with improved performance with respect to the baseline design and to POF designs obtained through a straightforward low-fidelity genetic optimization. Moreover, the proposed MFO strategy for SBO initialization is shown to be more effective than an SBO using a standard LHS initialization in producing blade geometries that represent a good trade-off between hover and forward flight performance. In summary, the proposed strategy appears to be a promising way for fast high-fidelity multi-point rotor blade design.

References

[1] B. Adams, K. Dalbey, M. Eldred, D. Gay, L. Swiler, W. Bohnhoff, J. Eddy, K. Haskell, P. Hough, DAKOTA, A Multilevel Parallel Object-Oriented Framework for Design Optimization, Parameter Estimation, Uncertainty Quantification, and Sensitivity Analysis. Version 5.0 User's Manual (2009).

[2] C. Allen, A. Morris, T. Rendall, Development of Generic CFD-Based Aerodynamic Optimisation Tools for Helicopter Rotor Blades, in: 25th AIAA Applied Aerodynamics Conference (2007).

[3] C. Allen, A. Morris, T. Rendall, CFD-Based Aerodynamic Shape Optimization of Hovering Rotors, in: 27th AIAA Applied Aerodynamics Conference (2009).

[4] C. Allen, A. Morris, T. Rendall, Computational-Fluid-Dynamics-Based Twist Optimization of Hovering Rotors, Journal of Aircraft 47 (2010).

[5] C. Allen, T. Rendall, CFD-based optimization of hovering rotors using radial basis functions for shape parameterization and mesh deformation, Optimization and Engineering 14 (2013) 97–118.

[6] G. Arnaud, B. Benoit, F. Toulmay, Improvements to the Aerodynamic Model of the R85 Helicopter Rotor Code Validation and Applications, in: 28th ISL Applied Aerodynamics Symposium (1991).

[7] P.M. Basset, R. Ormiston, Comparison and validation of the France/USA finite state rotor dynamic inflow models, in: 36th European Rotorcraft Forum (2010).

[8] P. Beaumier, M. Costes, B. Rodriguez, M. Poinot, B. Cantaloube, Weak and strong coupling between the elsA CFD solver and the HOST helicopter comprehensive analysis, in: 31th European Rotorcraft Forum (2005).

[9] M. Bebesel, G. Polz, E. Schöll, Aerodynamic and aeroacoustic layout of the ATR (Advanced Technology Rotor), in: 55th Annual Forum of the American Helicopter Society (1999).

[10] B. Benoit, A.M. Dequin, K. Kampa, W. Von Grünhagen, P.M. Basset, B. Gimonet, HOST, a General Helicopter Simulation Tool for Germany and France, in: 56th Annual Forum of the American Helicopter Society (2000).

[11] L. Cambier, S. Heib, S. Plot, The Onera elsA CFD software: input from research and feedback from industry, Mechanics & Industry (2013) 159–174.

[12] K. Collins, L. Sankar, Application of Low and High Fidelity Simulation Tools to Helicopter Rotor Blade Optimization, in: 65th Annual Forum of the American Helicopter Society (2009).

[13] S. Crary, Design of Computer Experiments for Metamodel Generation, Analog Integrated Circuits and Signal Processing 32 (2002) 7–16.

[14] A. Dumont, A. Le Pape, J. Peter, S. Huberson, Aerodynamic Shape Optimization of Hovering Rotors Using a Discrete Adjoint of the RANS equations, in: 65th Annual Forum of the American Helicopter Society (2009).

[15] K.T. Fang, R. Li, A. Sudjianto, Design and Modelling for Computer Experiments, Chapman & Hall/CRC Computer Science and Data Analysis Series, 2006.

[16] H. Glauert, A General Theory of the Autogyro, British ARC RM 1111 (1926).

[17] M. Imiela, High-fidelity optimization framework for helicopter rotors, Aerospace Science and Technology 1 (2011) 1–15.

[18] C. Johnson, G. Barakos, Optimising Aspects of Rotor Blades in Forward Flight, in: 49th AIAA Aerospace Sciences Meeting(2011).

[19] C. Johnson, G. Barakos, A Framework for the Optimisation of a BERP-like Blade, in: 51st AIAA Aerospace Sciences Meeting(2013).

[20] A. Le Pape, P. Beaumier, Numerical optimization of helicopter rotor aerodynamic performance in hover, Aerospace Science and Technology 9 (2005) 191–201.

[21] J.G. Leishman, Principles of Helicopter Aerodynamics, Cambridge University Press, second edition, 2006.

[22] D. Leusink, Advanced Numerical Tools for Aerodynamic Optimization of Helicopter Rotor Blades, Ph.D. thesis, Arts & Métiers ParisTech, 2013.

[23] D. Leusink, D. Alfano, P. Cinnella, Second order turbulence modelling for tip vortex computations: an industrial assessment, in: 46th Symposium of Applied Aerodynamics (2011).

[24] D. Leusink, D. Alfano, P. Cinnella, Aerodynamic rotor blade optimization at Eurocopter - a new way of industrial rotor blade design, in: 51st AIAA Aerospace Sciences Meeting(2013).

[25] M.S. Liou, A Sequel to AUSM: AUSM+, Journal of Computational Physics 129 (1996) 364–382.

[26] A. Massaro, A. D'Andrea, E. Benini, Multiobjective-Multipoint Rotor Blade Optimization in Forward Flight Conditions Using Surrogate-Assisted Memetic Algorithms, in: 37th European Rotorcraft Forum (2011).

[27] F.R. Menter, Improved Two-Equation k-omega Turbulence Models for Aerodynamic Flows, NASA Technical Memorandum 103975 (1992).

[28] M. Nemec, D.W. Zingg, T.H. Pulliam, Multipoint and Multi-Objective Aerodynamic Shape Optimization, AIAA Journal 42 (2004) 1057–1065.

[29] T. Simpson, T. Mauery, J. Korte, F. Mistree, Kriging Models for Global Approximation in Simulation-Based Multidisciplinary Design Optimization, AIAA Journal 39 (2001).

[30] L. Swiler, Gaussian Processes in Response Surface Modeling (2006).

[31] J. Walsh, G. Bingham, M. Riley, Optimization methods applied to the aerodynamic design of helicopter blades, NASA Technical Memorandum 89155 (1987).

[32] S. Yoon, A. Jameson, An LU-SSOR Scheme for the Euler and Navier-Stokes Equations, NASA Contractor Report 179556 (1986).

[33] A. Younis, Z. Dong, J. Gu, G. Li, Trends, Features, and Tests of Common and Recently Introduced Global Optimization Methods, in: 12th AIAA/ISSMO Multidisciplinary Analysis and Optimization Conference (2008).

[34] Q. Zhang, W. Liu, E. Tsang, B. Virginas, Expensive Multiobjective Optimization by MOEA/D with Gaussian Process Model, IEEE Transactions on Evolutionary Computation 14 (2010) 456–474.

[35] J. Zibi, G. Defresne, M. Costes, A numerical procedure for aerodynamic optimization of helicopter rotor blades, in: 18th European Rotorcraft Forum (1992), Avignon.